7-2009

DRAMMS: deformable registration via attribute matching and mutual-saliency weighting

Yangming Ou
University of Pennsylvania, ouya@seas.upenn.edu

Christos Davatzikos
University of Pennsylvania, christos@rad.upenn.edu

Yangming Ou, Christos Davatzikos, "DRAMMS: deformable registration via attribute matching and mutual-saliency weighting". Information Processing in Medical Imaging (IPMI), 2009: pp. 50-62.
The original publication is available at www.springerlink.com. DOI: 10.1007/978-3-642-02498-6_5

DRAMMS: deformable registration via attribute matching and mutual-saliency weighting

Abstract
A general-purpose deformable registration algorithm referred to as "DRAMMS" is presented in this paper. DRAMMS adds to the literature of registration methods that bridge between the traditional voxel-wise methods and landmark/feature-based methods. In particular, DRAMMS extracts Gabor attributes at each voxel and selects the optimal components, so that they form a highly distinctive morphological signature reflecting the anatomical context around each voxel in a multi-scale and multi-resolution fashion. Compared with intensity or mutual-information based methods, the high-dimensional optimal Gabor attributes render different anatomical regions relatively distinctively identifiable and therefore help establish more accurate and reliable correspondence. Moreover, the optimal Gabor attribute vector is constructed in a way that generalizes well, i.e., it can be applied to different registration tasks, regardless of the image contents under registration. A second characteristic of DRAMMS is that it is based on a cost function that weights different voxel pairs according to a metric referred to as "mutual-saliency", which reflects the uniqueness (reliability) of anatomical correspondences implied by the tentative transformation. As a result, image voxels do not contribute equally to the optimization process, as in most voxel-wise methods, or in a binary selection fashion, as in most landmark/feature-based methods. Instead, they contribute according to a continuously-valued mutual-saliency map, which is dynamically updated during the algorithm's evolution. The general applicability and accuracy of DRAMMS are demonstrated by experiments in simulated images, inter-subject images, single-/multi-modality images, and longitudinal images, from human and mouse brains, breast, heart, and prostate.

Keywords
image registration, deformable registration, non-rigid registration, Gabor filter bank, general-purpose, mutual-saliency

Disciplines
Bioimaging and Biomedical Optics

Comments
Yangming Ou, Christos Davatzikos, "DRAMMS: deformable registration via attribute matching and mutual-saliency weighting". Information Processing in Medical Imaging (IPMI), 2009: pp. 50-62.

The original publication is available at www.springerlink.com. DOI: 10.1007/978-3-642-02498-6_5

DRAMMS: Deformable Registration via Attribute Matching and Mutual-Saliency Weighting

Yangming Ou and Christos Davatzikos

Section of Biomedical Image Analysis (SBIA),
University of Pennsylvania, Philadelphia, PA, 19104
{Yangming.Ou,Christos.Davatzikos}@uphs.upenn.edu

Abstract. A *general-purpose* deformable registration algorithm referred to as "DRAMMS" is presented in this paper. DRAMMS adds to the literature of registration methods that bridge between the traditional voxel-wise methods and landmark/feature-based methods. In particular, DRAMMS extracts Gabor attributes at each voxel and selects the optimal components, so that they form a highly distinctive morphological signature reflecting the anatomical context around each voxel in a multi-scale and multi-resolution fashion. Compared with intensity or mutual-information based methods, the high-dimensional optimal Gabor attributes render different anatomical regions relatively distinctively identifiable and therefore help establish more accurate and reliable correspondence. Moreover, the optimal Gabor attribute vector is constructed in a way that generalizes well, i.e., it can be applied to different registration tasks, regardless of the image contents under registration. A second characteristic of DRAMMS is that it is based on a cost function that weights different voxel pairs according to a metric referred to as "mutual-saliency", which reflects the uniqueness (reliability) of anatomical correspondences implied by the tentative transformation. As a result, image voxels do not contribute equally to the optimization process, as in most voxel-wise methods, or in a binary selection fashion, as in most landmark/feature-based methods. Instead, they contribute according to a continuously-valued mutual-saliency map, which is dynamically updated during the algorithm's evolution. The general applicability and accuracy of DRAMMS are demonstrated by experiments in simulated images, inter-subject images, single-/multi-modality images, and longitudinal images, from human and mouse brains, breast, heart, and prostate.

1 Introduction

Deformable registration is the building block for a variety of medical image analysis tasks, such as multi-modality information fusion, atlas-based image segmentation and computational anatomy. Existing deformable registration methods can be generally classified into two main categories: voxel-wise methods (e.g., [1,2,3,4,5,6,7]) and landmark/feature-based methods (e.g., [8,9,10,11,12,13,14]).

J.L. Prince, D.L. Pham, and K.J. Myers (Eds.): IPMI 2009, LNCS 5636, pp. 50–62, 2009.

While landmark/feature-based methods are more intuitive (in the sense that they often explicitly detect and establish correspondence on those anatomically salient regions), they often suffer from the inevitable errors in the landmark/feature detection and matching processes. Moreover, they only utilize a small subset of imaging data (e.g., corner, boundary, line intersection), in a way that is often *ad hoc* and dependent on the specific image contents under registration. For those reasons, recent literature on general-purpose registration has mostly focused on voxel-wise methods, which usually equally utilize all imaging data and maximize the overall similarity on certain voxel-wise attributes (e.g., intensities, intensity distributions). However, voxel-wise methods usually have limitations in the following two respects.

First, the attributes used for characterizing voxels are often not optimal. Since the matching between a pair of voxels is usually determined by the matching between their attributes, suboptimal attributes often lead to ambiguities in matching [15,30]. Ideally, an optimal set of attributes should satisfy two conditions: 1) discriminative, i.e., attributes of voxels from the two images should be similar if and only if those voxels are anatomically corresponding to each other, therefore leaving minimum ambiguity in matching; 2) generally applicable, i.e., they can be extracted from any image while satisfying the first condition, regardless of the image contents under registration. However, most voxel-wise methods only use the simple attribute of image intensity, which is generally applicable for diverse registration tasks but often not sufficiently discriminative for matching (for instance, hundreds of thousands of gray matter voxels in a brain image would have similar intensities; but they may all correspond to different anatomical regions). Other methods attempt to reduce matching ambiguities (e.g., [11,30]) by using a richer set of attributes, such as sulci, organ boundaries, tissue membership and tensor orientations. Those attributes, although more discriminative for matching, are often task- and parameter- specific.

Second, equally utilizing all imaging data may undermine the performance of the optimization process. Actually, different anatomical regions/voxels usually have different abilities to establish unique correspondence [16,17,18]. An ideal optimization process should weight more on those regions/voxels having higher abilities to establish unique correspondences across images. For instance, Fig. 1 shows three similarity maps (Fig. 1(c)(d)(e)) between one specific voxel (red, blue or orange) in the subject image and all the voxels in the template image. An ideal optimization process should rely more on the red point, then the blue point, and lastly the orange point. Unfortunately, most voxel-wise methods treat all voxels equally, ignoring such differences; other approaches (e.g. [11]) attempted to address this issue, by driving the registration adaptively/hierarchically using certain anatomically salient regions, however, in their approaches voxels are often utilized in a heuristic and binary way, ignoring the potential contributions from other voxels that are not utilized.

This paper presents a *general-purpose* image registration framework referred to as "DRAMMS" – Deformable Registration via Attribute Matching and Mutual-Saliency weighting. To overcome the first limitation, DRAMMS extracts a rich set

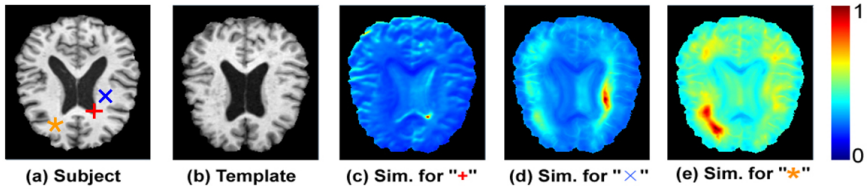

Fig. 1. Demonstration of the importance of weighting voxels continuously, as they often have different abilities to establish unique correspondence. Similarity maps (c-e) are generated between one specific voxel in image (a) to all voxels in image (b). The red point should have higher weight than the blue point, then the orange point.

of multi-scale and multi-orientation Gabor attributes at each voxel and automatically selects the optimal attribute components. The optimal Gabor attributes render it relatively robust in attribute-based image matching and are also constructed in a way that is generalizable to diverse problems, organs and image modalities. To overcome the second limitation, DRAMMS continuously weights voxels during the optimization process, based on a function referred to as "mutual-saliency", which measures the uniqueness (hence reliability) of a tentative correspondence implied by the transformation. Instead of equally treating voxels or isolating voxels that have more distinctive attributes, this mutual-saliency based continuous weighting mechanism utilizes all imaging data with appropriate and dynamically-evolving weights and leads to a more effective optimization process. DRAMMS is elaborated in Section 2 and demonstrated in Section 3. The whole paper is concluded in Section 4.

2 Methods

2.1 Formulation

Given two intensity images $I_1 : \Omega_1 \mapsto \mathbb{R}$ and $I_2 : \Omega_2 \mapsto \mathbb{R}$ in the 3D image domains $\Omega_i (i = 1, 2) \subset \mathbb{R}^3$, DRAMMS seeks a transformation T that maps every voxel $\mathbf{u} \in \Omega_1$ to its counterpart $T(\mathbf{u}) \in \Omega_2$, by minimizing an overall cost function $E(T)$,

$$\min_T E(T) = \int_{\mathbf{u}\in\Omega_1} w\left(\mathbf{u}, T(\mathbf{u})\right) \cdot \|A_1^\star(\mathbf{u}) - A_2^\star\left(T(\mathbf{u})\right)\|^2 d\mathbf{u} \; + \; \lambda R(T) \qquad (1)$$

where $A_i^\star(\cdot)\ (i = 1, 2)$ is the optimal attribute vector that reflects the geometric and anatomical context around each voxel. By minimizing $\|A_1^\star(\mathbf{u}) - A_2^\star\left(T(\mathbf{u})\right)\|^2$, we seek a transformation T that minimizes the *dis*similarity between a pair of voxels $\mathbf{u} \in \Omega_1$ and $T(\mathbf{u}) \in \Omega_2$. The derivation of the optimal attribute vector $A_i^\star(\cdot)\ (i = 1, 2)$ will be discussed in Sections 2.2 and 2.3.

$w\left(\mathbf{u}, T(\mathbf{u})\right)$ is a continuous weight that is calculated from the mutual-saliency of $\mathbf{u} \in \Omega_1$ and $T(\mathbf{u}) \in \Omega_2$ – higher uniqueness of their matching in the neighborhood indicates higher mutual-saliency, and hence higher weight in the optimization process. In contrast, most traditional voxel-wise methods use equal weights ($w(\cdot) \equiv 1$). The definition of mutual-saliency will be discussed in Section 2.4.

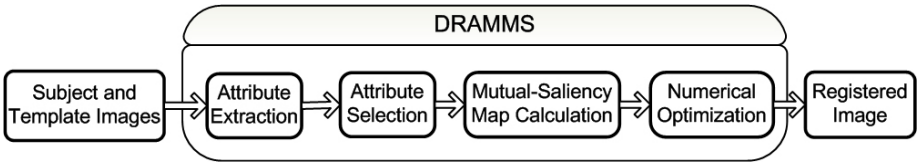

Fig. 2. The components of DRAMMS

$R(T)$ is a smoothness/regularization term usually corresponding to the Laplacian operator, or the bending energy[19], of the deformation field T, whereas λ is a balancing parameter that controls the extent of smoothness.

Fig. 2 illustrates the components of DRAMMS. Details for each component are elaborated in the subsequent sections.

2.2 Attribute Extraction

DRAMMS extracts Gabor attributes at each voxel by convolving the images under registration with Gabor filter banks. The use of Gabor attributes is mainly motivated by the following three properties of Gabor filter banks:

1) General applicability and successful application in numerous tasks. As a general-purpose registration framework, DRAMMS must extract attributes that are generally applicable to different registration tasks, regardless of the image contents. Fortunately, almost all anatomical images have texture information, at some scale and orientation, reflecting the underlying geometric and anatomical characteristics. This texture can be effectively captured by Gabor attributes, as demonstrated in a variety of studies, including texture segmentation [21], image retrieval [23], cancer detection [22] and prostate tissue differentiation [24]. Recently, Gabor attributes have been successfully used in [25][26][27] to register different images, showing their promise for diverse image registration tasks. These methods have also noted the high computational cost required by the high-dimensional Gabor attributes and the need for optimally using Gabor attributes. These challenges are dealt with in DRAMMS by an attribute selection method, as discussed in Section 2.3.

2) Suitability for single- and multi-modality registration tasks. The multi-scale Gabor filter banks often cover a wide range of frequencies, where low frequency filters often serve as local image smoothers, and high frequency filters often serve as edge-detectors. The detected edge information is, to some extent, independent from the underlying intensity distributions, and is therefore suitable for multi-modality registration tasks, even when intensity distributions in the two images no longer follow consistent relationship, in which case mutual-information [7] based methods may fail [25];

3) Multi-scale and multi-orientation nature. As scale and orientation are closely related to the distinctiveness of attributes [28], the multi-scale and multi-orientation attributes are more likely to render each voxel distinctively identifiable, therefore reducing ambiguities in attribute-based voxel matching.

Following the work in [24], the 3D Gabor attributes at each voxel are approximated by convolving the 3D image with two 2D Gabor filter banks in two orthogonal planes (x-y and y-z), so as to save computational cost. Mathematically, the two 2D Gabor filter banks in two orthogonal planes are

$$g_{m,n}(x,y) = a^{-m} g\left(a^{-m}x_g^{'}, a^{-m}y_g^{'}\right),\ h_{m,n}(y,z) = a^{-m} h\left(a^{-m}y_h^{'}, a^{-m}z_h^{'}\right) \quad (2)$$

where a is the scale factor, $m = 1, 2, \ldots, M$ is the scale index, with M being the total number of scales; $x_g^{'} = x\cos\left(\frac{n\pi}{N}\right) + y\sin\left(\frac{n\pi}{N}\right)$, $y_g^{'} = -x\sin\left(\frac{n\pi}{N}\right) + y\cos\left(\frac{n\pi}{N}\right)]$, $y_h^{'} = y\cos\left(\frac{n\pi}{N}\right) + z\sin\left(\frac{n\pi}{N}\right)$ and $z_h^{'} = -y\sin\left(\frac{n\pi}{N}\right) + z\cos\left(\frac{n\pi}{N}\right)$ are rotated coordinates, where $n = 1, 2, \ldots, N$ is the orientation index, with N being the total number of orientations. $g(x,y)$ and $h(y,z)$, known as the "mother Gabor filters", are complex-valued functions in the spatial domain and are each obtained by modulating a Gaussian envelope with a complex exponential,

$$g(x,y) = \frac{1}{2\pi\sigma_x\sigma_y}\exp\Big[\underbrace{-\frac{1}{2}\left(\frac{x^2}{\sigma_x^2} + \frac{y^2}{\sigma_y^2}\right)}_{\text{Gaussian Envelope}} + j2\pi f_x\Big]; \quad (3)$$

$$h(y,z) = \frac{1}{2\pi\sigma_y\sigma_z}\exp\Big[\underbrace{-\frac{1}{2}\left(\frac{y^2}{\sigma_y^2} + \frac{z^2}{\sigma_z^2}\right)}_{\text{Gaussian Envelope}} + j2\pi f_y\Big] \quad (4)$$

where σ_x, σ_y and σ_z are the semi-axes lengths of the Gaussian envelope in the spatial domain; f_x and f_y are modulating (shifting) factors in the frequency domain (often known as "central frequencies"). Therefore, at each voxel (x,y,z) in the image $I_i (i = 1, 2)$, the approximated 3D Gabor attributes are assembled into a $D = M \times N \times 4$ dimensional attribute vector $\tilde{A}_i(x,y,z)$, from which we can select the optimal components.

$$\begin{aligned}\tilde{A}_i(x,y,z) = \big[\ & (I_i * g_{m,n})_{\mathrm{Re}}(x,y),\ (I_i * g_{m,n})_{\mathrm{Im}}(x,y), \\ & (I_i * h_{m,n})_{\mathrm{Re}}(y,z),\ (I_i * h_{m,n})_{\mathrm{Im}}(y,z)\ \big]_{m=1,2,\ldots,M;\ n=1,2,\ldots,N.}\end{aligned} \quad (5)$$

2.3 Attribute Selection

A disadvantage of Gabor attributes is the redundancy among attributes, which is caused by the non-orthogonality among Gabor filters at different scales and orientations. This redundancy not only increases computational cost, but more importantly, it may reduce the distinctiveness of attribute representation, causing ambiguities in the attribute matching [23]. It is therefore important to design a learning-based method to select a set of optimal Gabor attributes so that voxels from the two images can be *accurately* and *reliably* matched.

To design such a learning-based attribute selection method, we would ideally need some *a priori* knowledge of a number of anatomically corresponding voxel pairs to serve as ground-truth, or training voxel pairs. However, in the context

of a general-purpose algorithm, this kind of *a priori* knowledge is often absent. Therefore, DRAMMS first automatically selects training voxel pairs, then based on them selects the optimal attributes. These two steps are respectively described below.

Selecting Representative Training Voxel Pairs

The training voxel pairs should 1) be representative of all other voxels in the entire image domain; and 2) offer examples of good correspondence. Accordingly, DRAMMS regularly partitions the subject image into a number of J regions $\Omega_1^{(j)}(j = 1, 2, \ldots, J)$ and selects from each region a voxel pair $(\mathbf{p}_j^\star \in \Omega_1^{(j)}, \mathbf{q}_j^\star \in \Omega_2)$ that is most *reliably* matched to each other, as illustrated in Fig. 3 and mathematically described in Eqn. 6. Here regular partition is used instead of more complicated organ/tissue segmentation, in order to keep DRAMMS as a general-purpose registration method that can be applied to different registration tasks without assumptions on segmentation. Note also that the template image I_2 is not partitioned because at this stage, no transformation is performed and no corresponding regions should be assumed.

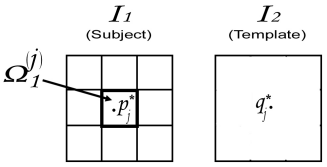

Fig. 3. Illustration of the selection of representative training voxel pairs. Please refer to text for details.

$$\left(\mathbf{p}_j^*, \mathbf{q}_j^*\right) = \arg \max_{\substack{\mathbf{p}\in\Omega_1^{(j)}\subset\Omega_1,\\ \mathbf{q}\in\Omega_2}} \Big[\underbrace{w(\mathbf{p},\mathbf{q})}_{\text{Reliability}} \cdot \underbrace{sim\left(\tilde{A}_1(\mathbf{p}), \tilde{A}_2(\mathbf{q})\right)}_{\text{Similarity}} \Big] \tag{6}$$

In Eqn. 6, $sim\big(\tilde{A}_1(\mathbf{p}), \tilde{A}_2(\mathbf{q})\big) = \frac{1}{1+\frac{1}{D}\|\tilde{A}_1(\mathbf{p})-\tilde{A}_2(\mathbf{q})\|^2} \in [0,1]$ reflects the attribute-wise similarity between the two points, with D being the number of attributes. $w(\mathbf{p},\mathbf{q})$, the mutual-saliency, is elaborated in Section 2.4. For now, the bottom line is that $w(\mathbf{p},\mathbf{q})$ reflects the uniqueness (hence reliability) of the matching between $\mathbf{p} \in \Omega_1$ and $\mathbf{q} \in \Omega_2$.

Selecting Optimal Attributes. DRAMMS selects a subset of optimal attributes, $A_1^\star$ and $A_2^\star$, such that they maximize the overall *reliability* and *similarity* of the matching on those selected training voxel pairs,

$$\max_{A_1\subset\tilde{A}_1,\, A_2\subset\tilde{A}_2} \sum_{j=1}^{J} \Big[\underbrace{w(\mathbf{p}_j^\star, \mathbf{q}_j^\star)}_{\text{Reliability}} \cdot \underbrace{sim\left(A_1(\mathbf{p}_j^\star), A_2(\mathbf{q}_j^\star)\right)}_{\text{Similarity}} \Big] \tag{7}$$

In implementation, DRAMMS adopts an iterative backward elimination and forward inclusion strategy for attribute selection, which are commonly used for attribute/variable selection in the machine learning community [29]. Note that, in order to make the quantity in Eqn. 7 comparable for different numbers of attributes, the difference between two attribute vectors $||A_1(\mathbf{p}^\star) - A_2(\mathbf{q}^\star)||^2$ in the definition of $sim\left(A_1(\mathbf{p}_j^\star), A_2(\mathbf{q}_j^\star)\right)$ is normalized by the number of attributes.

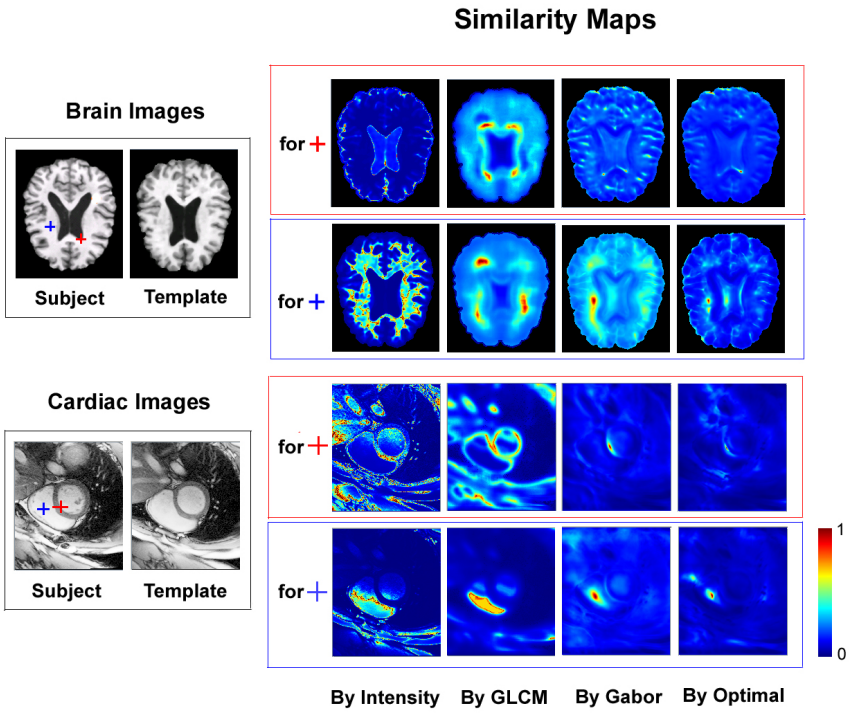

Fig. 4. Role of attribute selection in reducing matching ambiguities, as illustrated on special voxels (red crosses) and ordinary voxels (blue crosses) in brain and cardiac images of different individuals. Similarity maps are generated between a voxel (red or blue) in the subject image and all voxels in the template image. "GLCM", gray-level co-occurrence matrix [20], is another commonly used texture attribute descriptor.

Role of Optimized Gabor Attributes. Fig. 4 shows that the optimized Gabor attributes lead to highly distinctive attribute similarity maps between the subject and the template brain and cardiac images, for two voxels in each case. This reduces the computational cost and the ambiguities in matching. In particular, since the similarity function for a given voxel now looks more like a delta function, the optimal Gabor attributes are likely to reduce local minima and therefore assist the optimization process to converge to the global minimum.

2.4 Using Mutual-Saliency Map to Modulate Registration

As addressed in the introduction, an ideal optimization process should utilize all voxels but assign a continuously-valued weight to each voxel, based on whether a reliable correspondence could be established at this voxel.

Previous work [30][31] assumed that more *salient* regions could establish more *reliable* correspondence and hence should be assigned with higher weights. They have reported improved registration accuracies. However, this assumption does

not always hold, as regions that are salient in one image are not necessarily salient in the other image, or do not necessarily have unique correspondence across images, especially in convoluted and complex structures such as the human brain cortex. In other words, saliency in one image does not necessarily indicate matching reliability between two images.

To measure matching reliability (uniqueness) between two images, DRAMMS extends the concept of *saliency*, which is often observed in one image, to the concept of *mutual-saliency*, which, as manifested in Fig. 5, is directly defined on a pair of voxels in the two images under registration. In particular, a pair of voxels $\mathbf{u} \in \Omega_1$ and $T(\mathbf{u}) \in \Omega_2$ is defined to have high mutual-saliency $ms\left(A_1(\mathbf{u}), A_2(T(\mathbf{u}))\right)$ and hence should be assigned with high weight $w\left(\mathbf{u}, T(\mathbf{u})\right)$, if $\mathbf{u}$ has high similarity to voxels in the core neighborhood of $T(\mathbf{u})$ and low similarity to voxels far away from $T(\mathbf{u})$,

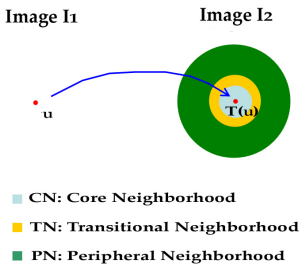

Fig. 5. Illustration of the definition of mutual-saliency function. Refer to text for details.

$$w\left(\mathbf{u}, T(\mathbf{u})\right) = ms\big(A_1(\mathbf{u}), A_2(T(\mathbf{u}))\big) = \frac{MEAN_{\mathbf{v}\in CN(T(\mathbf{u}))}\ \big[sim\big(A_1(\mathbf{u}), A_2(\mathbf{v})\big)\big]}{MEAN_{\mathbf{v}\in PN(T(\mathbf{u}))}\ \big[sim\big(A_1(\mathbf{u}), A_2(\mathbf{v})\big)\big]} \tag{8}$$

where $sim(\cdot,\cdot)$ is defined in the same way as in Eqns. 6 and 7. Note that voxels in between the core and peripheral neighborhoods of $T(\mathbf{u})$ are ignored because there is typically a smooth transition from high to low similarities, especially for coarse-scale Gabor attributes. For the same reason, the radii of those neighborhoods are adaptive to the scale in which Gabor attributes are extracted.

Roles of Mutual-Saliency Maps. 1) *Missing data*: the mutual-saliency map effectively identifies regions in which no good correspondence can be found and reduces their negative impact. In Fig. 6, motivated by our work on matching histological sections with MRI, we have simulated cross-shaped tears in the subject image, which are typical when sections are stitched together. Mutual-saliency

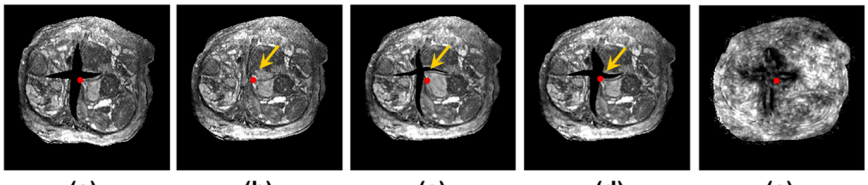

Fig. 6. Role of mutual-saliency map in accounting for partial loss of correspondence. (a) Subject image, with simulated deformation and tears from (b) template image. (c, d) Registered images without and with using mutual-saliency map; (e) Mutual-saliency map associated with (d). Red points denote the same spatial locations in all sub-figures.

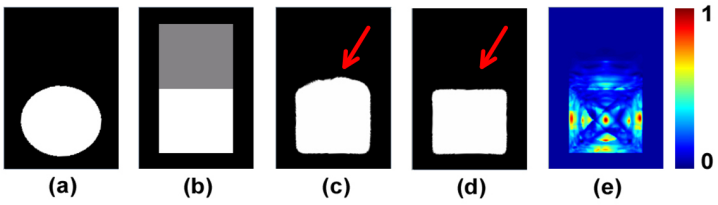

Fig. 7. Role of mutual-saliency map in reducing the negative impact of matching ambiguities. (a) Subject image; (b) Template image; (c,d) Registered images, without and with using mutual-saliency map; (e) Mutual-saliency map associated with (d).

map assigns low weights to the tears, therefore reducing their negative impacts towards the registration process. On the contrary, registration process without using mutual-saliency map tends to fill in the tears by aggressively pulling other regions, causing inaccurate results, as pointed out by the arrows in Fig. 6(c); **2)** *Matching ambiguities*: even without loss of correspondences, mutual-saliency map can accurately identify regions having matching ambiguities and reduce their negative impact. In Fig. 7, the mutual saliency map assigns highest weights to those regions that have minimum ambiguity in matching (e.g., the center, the left, right and bottom edge of the circular plate in Fig. 7(a)). Meanwhile, regions that have considerable ambiguity in matching (e.g., the top edge of the circular plate) are correctly assigned with low weights; therefore their negative impact is minimized and a desirable registration result is obtained, as shown in Fig. 7(d).

2.5 Numerical Optimization

DRAMMS was optimized using free form deformation (FFD) model, which has been widely used in deformable registration community, and was implemented using gradient descent and line search strategies in a multi-resolution fashion, so as to reduce the risk of being trapped at local minima. Following standard FFD model, the transformation field is regularized by its "bending energy" [6,19], and the distance between the control points is chosen at 7 voxels in $x-y$ directions and 2 voxels in z direction. All experiments were operated in C code on a 2.8

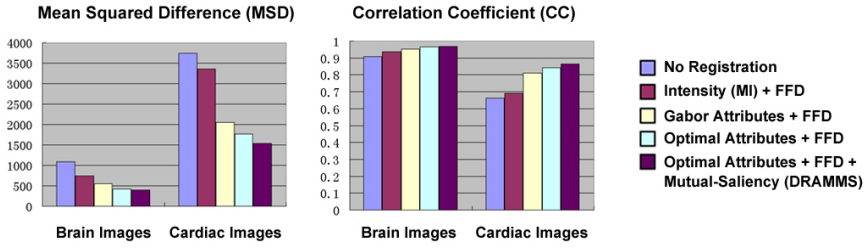

Fig. 8. Quantitative evaluation of the registration accuracies of inter-subject brain and cardiac images, in terms of MSD and CC between registered and template images. Each of DRAMMS' components provides additive improvement over MI-based FFD.

G Intel Xeon processor with UNIX operation system. Registering two 2D slices (256×256) typically costs about 80 seconds and registering two 3D images ($256 \times 256 \times 30$) typically costs about 25 minutes.

3 Results

As a general-purpose registration method, DRAMMS has been tested extensively in diverse registration tasks and on different organs, and has been compared with mutual information (MI)-based FFD, another commonly used general-purpose registration method. Note that, the default set of parameters is used for MI-based FFD as provided in MIPAV, a public software package [32]. To be fair, DRAMMS also used a single set of parameters throughout the comparisons.

3.1 Simulated Images. Registration results for simulated images have already been shown in Figs. 6 and 7. Largely due to the mutual-saliency component, DRAMMS outperforms MI-based FFD in both experiments.

3.2 Inter-Subject Registration. Brain and cardiac images of different individuals (the ones shown in the left column of Fig. 4) have been registered by different methods. Registration results are quantitatively compared in terms of mean squared difference (MSD) and correlation coefficient (CC) between the registered and the template images. Since the images under registration are of the same modality, high registration accuracy normally corresponds to decreased MSD and increased CC. As shown in Fig. 8, each of DRAMMS' components provides additive improvement of registration accuracy over MI-based FFD.

3.3 Multi-modality Registration. In Fig. 9, histological images of mouse brain and human prostate are registered to MR images of the same subject in order to map histologically-defined tumor ground truth onto MR space. Due

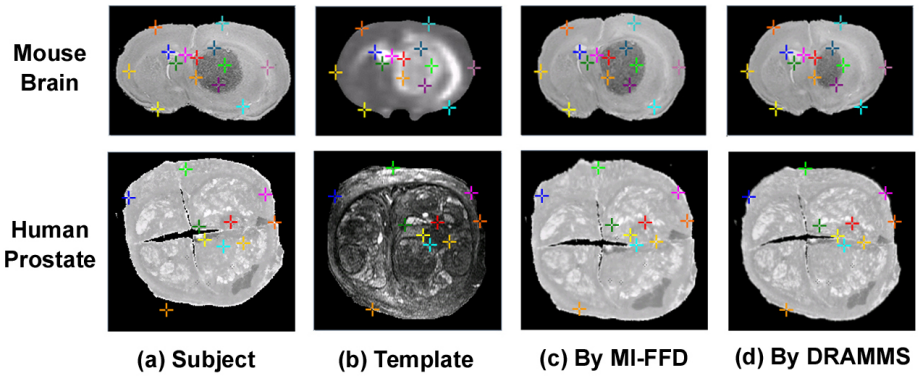

Fig. 9. Multi-modality registration on mouse brain and human prostate between (a) histological and (b) MR images, by (c) MI-based FFD and (d) DRAMMS. In each case (row), crosses of the same color denote the same spatial locations in all images.

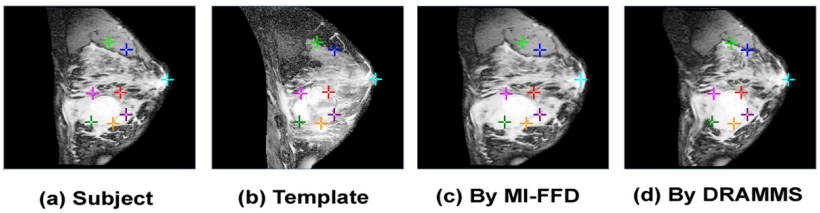

Fig. 10. Longitudinal registration of breast images, between (a) subject (baseline) and (b) template (follow-up) images, with results generated by (c) MI-based FFD and (d) DRAMMS. Crosses of the same color denote the same locations in all images

to the greatly different imaging characteristics between the two modalities, their intensity distributions do not follow consistent relationship, violating the underlying assumption of MI-based methods, so theoretically it is not surprising that MI-based methods tend to fail. To make things worse, registration is also challenged by the partial loss of correspondence caused by the stitching effects in the histology (as in the prostate case). For the same reasons, registration accuracy could no longer be evaluated by MSD or CC. Instead, crosses of the same colors have been placed at the same spatial locations in each sub-figure, in order to visually reveal whether the anatomical structures have been successfully aligned. Compared with MI-based FFD, DRAMMS is able to align tumor and other complicated structures.

3.4 Longitudinal Registration. In Fig. 10, a baseline MR image is registered to a follow-up MR image of the same breast to study the tumor change. Even though the two images are of the same modality, it is not difficult to observe that their intensity distributions, to some extent, no longer follow a consistent relationship, largely due to the unpredictable changes of tumor in size and shape, and the projection differences caused by changes in positioning of the subject during image acquisition. Consequently, it is also not surprising that, in this case, MI-based method is severely challenged or even tends to fail. In contrast, DRAMMS captures tumor changes, although still not perfectly.

4 Conclusions

We have presented a *general-purpose* deformable registration method referred to as "DRAMMS", which makes primarily two contributions. First, DRAMMS attaches a Gabor attribute vector to each image voxel, which serves as a morphological signature of the anatomy around that voxel. By optimizing these attributes using an automated attribute selection method, it produces highly unique (hence reliable) matching, which potentially helps reduce local minima that are prevalent in intensity-based matching methods. Second, DRAMMS modulates the optimization process by a continuously-valued weighting function derived from "mutual-saliency". Mutual-saliency maps assign lower weights to regions having

difficulties establishing reliable correspondences, therefore reducing the negative impacts caused by the matching ambiguities and/or the partial loss of correspondence. The general applicability and accuracy of DRAMMS are demonstrated in diverse registration tasks, including simulated images, inter-subject images, single- and multi-modality images and longitudinal images, on human and mouse brains, heart, breast and prostate. In images that the traditional mutual information-based free form deformation (MI-based FFD) method could register, DRAMMS has obtained slightly higher registration accuracy; while in images where the MI-based FFD method tended to fail, DRAMMS has provided significant improvement.

References

1. Glocker, B., et al.: Dense image registration through MRFs and efficient linear programming. Medical Image Analysis 12(6), 731–741 (2008)
2. Vercauteren, T., et al.: Non-parametric Diffeomorphic Image Registration with the Demons Algorithm. In: Ayache, N., Ourselin, S., Maeder, A. (eds.) MICCAI 2007, Part II. LNCS, vol. 4792, pp. 319–326. Springer, Heidelberg (2007)
3. Christensen, G.E., Rabbitt, R.D., Miller, M.I.: 3D brain mapping using a deformable neuroanatomy. Phys. Medicine Biol. 39, 609–618 (1994)
4. Collins, D.L., et al.: Automatic 3D intersubject registration on MR volumetric data in standardized talairach space. J. Comput. Assist. Tomogr. 18(2), 192–205 (1994)
5. Thirion, J.-P.: Image matching as a diffusion process: An analogy with maxwells demons. Med. Image Anal. 2(3), 243–260 (1998)
6. Rueckert, D., et al.: Nonrigid registration using free-form deformations: Application to breast MR images. IEEE Trans. Med. Imag. 18(8), 712–721 (1999)
7. Wells III, W.M., et al.: Multi-modal volume registration by maximization of mutual information. Medical Image Analysis 1(1), 35–51 (1996)
8. Davatzikos, C., Prince, J.L., Bryan, R.N.: Image registration based on boundary mapping. IEEE Trans. on Med. Imag. 15(1), 112–115 (1996)
9. Thompson, P., Toga, A.: Anatomically-driven strategies for high-dimensional brain image warping and pathology detection. Brain Warping, 311–336 (1998)
10. Rohr, K., et al.: Landmark-based elastic registration using approximating thin-plate splines. IEEE Trans. Med. Imaging 20(6), 526–534 (2001)
11. Shen, D., Davatzikos, C.: HAMMER: Hierarchical Attribute Matching Mechanism for Elastic Registration. IEEE Trans. Med. Imaging 21(11), 1421–1439 (2002)
12. Joshi, S.C., Miller, M.I.: Landmark matching via large deformation diffeomorphisms. IEEE Trans. Image Processing 9, 1357–1370 (2000)
13. Chui, H., Rangarajan, A.: A new point matching algorithm for non-rigid registration. Computer Vision Image Understanding 89, 114–141 (2003)
14. Zhan, Y., et al.: Registering Histologic and MR Images of Prostate for Image-based Cancer Detection. Academic Radiology 14(11), 1367–1381 (2007)
15. Xue, Z., Shen, D., Davatzikos, C.: Determining correspondence in 3-D MR brain images using attribute vectors as morphological signatures of voxels. IEEE Trans. Med. Imag. 23(10), 1276–1291 (2004)
16. Anandan, P.: A computational framework and an algorithm for the measurement of visual motion. Int. J. Comput. Vision 2, 283–310 (1989)
17. McEachen II, J.C., Duncan, J.: Shape-Based Tracking of Left Ventricular Wall Motion. IEEE Trans. Med. Imaging 16(3), 270–283 (1997)

18. Wu, G., Qi, F., Shen, D.: Learning Best Features and Deformation Statistics for Hierarchical Registration of MR Brain Images. In: Karssemeijer, N., Lelieveldt, B. (eds.) IPMI 2007. LNCS, vol. 4584, pp. 160–171. Springer, Heidelberg (2007)
19. Bookstein, F.L.: Principal warps: Thin-Plate splines and the decomposition of deformations. IEEE Trans. Pattern Anal. Mach. Intell. 11(6), 567–585 (1989)
20. Haralick, R.M.: Statistical and structural approaches to texture. Proc. IEEE 67(5), 786–804 (1979)
21. Jain, A.K., Farrokhnia, F.: Unsupervised texture segmentation using Gabor filters. Pattern Recognition 24(12), 1167–1186 (1991)
22. Zhang, J., Liu, Y.: Cervical Cancer Detection Using SVM Based Feature Screening. In: Barillot, C., Haynor, D.R., Hellier, P. (eds.) MICCAI 2004. LNCS, vol. 3217, pp. 873–880. Springer, Heidelberg (2004)
23. Manjunath, B.S., Ma, W.Y.: Texture features for browsing and retrieval of image data. IEEE Trans. Pattern Anal. Mach. Intell. 18(8), 837–842 (1996)
24. Zhan, Y., Shen, D.: Deformable Segmentation of 3D Ultrasound Prostate Images Using Statistical Texture Matching Method. IEEE TMI 25, 256–272 (2006)
25. Liu, J., Vemuri, B.C., Marroquin, J.L.: Local frequency representations for robust multimodal image registration. IEEE Trans. on Med. Imag. 21, 462–469 (2002)
26. Verma, R., Davatzikos, C.: Matching of Diffusion Tensor Images using Gabor Features. In: ISBI, pp. 396–399 (2004)
27. Elbakary, M., Sundareshan, M.K.: Accurate representation of local frequency using a computationally efficient Gabor filter fusion approach with application to image registration. Pattern Recognition Letters 26(14), 2164–2173 (2005)
28. Kadir, T., Brady, M.: Saliency, scale and image description. Int. J. Comput. Vision 45(2), 83–105 (2001)
29. Fan, Y., et al.: COMPARE: Classification of Morphological Patterns Using Adaptive Regional Elements. IEEE Trans. Med. Imaging 26(1), 93–105 (2007)
30. Wu, G., Qi, F., Shen, D.: Learning-based deformable registration of MR brain images. IEEE Trans. Med. Imaging 25(9), 1145–1157 (2006)
31. Mahapatra, D., Sun, Y.: Registration of dynamic renal MR images using neurobiological model of saliency. IEEE ISBI, 1119–1122 (2008)
32. McAuliffe, M., et al.: Medical image processing, analysis and visualization in clinical research. In: Proc. 14th IEEE Comp. Based Med. Sys., pp. 381–386 (2001)